High Level and Dual Level Direct Dynamics in the Intramolecular Proton Transfer of Hydrogenoxalate Anion. Influence of Tunneling and Isotopic Effect

Antonio Fernández-Ramos, Jesús Rodríguez-Otero, and Miguel A. Ríos*

Departamento de Química Física, Facultade de Química, Universidade de Santiago de Compostela, E 15706 Santiago de Compostela, Spain

Received: November 19, 1997; In Final Form: February 2, 1998

Direct ab initio dynamics methodology was used to investigate intramolecular proton transfer in hydrogenoxalate anion and its deuterated species. The method used is based on the variational theory of the transition state as modified by introducing semiclassical corrections for the estimation of tunneling on the sole basis of electronic structure calculations. Such calculations, which included energies, gradients, and Hessians, both at stationary points and throughout the reaction path, were done by using the MP2/6-31++G** level with barrier height corrections at QCISD/6-31++G** (4.85 kcal/mol). No variational effects were observed at this fairly high computational level over the temperature range studied. Some of the modes of this reaction are highly coupled to the reaction path, so tunneling may be quite substantial. Within the direct ab initio dynamics we used the small curvature approximation (SCT) to assess tunneling; however, because the particle transferred is a light particle, the problem may call for an approximation that considers a more rectilinear path for the proton. Such is the case with the large curvature approximation (LCT). We had calculated the LCT transmission factors as well as the SCT transmission factors within the dual level dynamics, replacing ab initio calculations in the nonstationary points by a semiempirical method, which was previously parametrized for this kind of system. The results of high level and dual level calculations were quite consistent. Also, the SCT approximation was found to describe tunneling more accurately than did the LCT treatment, partly as a result of the low transfer barrier involved. The analysis of contributions to kinetic isotopic effect revealed that, although tunneling contributes significantly, vibration is the single most influential factor in this respect.

1. Introduction

Proton-transfer reactions are of high interest on account of their occurrence in a variety of chemical and biological processes.[1−4] These reactions, which involve the transfer of a light particle, are usually subject to nonclassical effects such as tunneling. As a result, their study requires a deep knowledge of the potential energy surface (PES) for the process concerned. The use of analytical PES for examining reactions is usually cumbersome and computationally expensive and entails the prior knowledge of the more significant aspects of the process dynamics. Methods based exclusively on electronic structure calculations (energies, gradients, and Hessians) are of enormous assistance in this context as they allow the examination of dynamic aspects of a reaction with none of the constraints of an analytical PES. This recent methodological approach is usually referred to as *direct dynamics.*[5−10] In this work, direct dynamics calculations based on the variational theory of the transition state (VTST) that included semiclassical corrections for tunneling[11,12] were performed. One major usual constraint of direct dynamics calculations is the high computational cost of electronic structure calculations, which can be minimized by using appropriate semiempirical methods. However, most such methods require adaptation of their parameters to the reaction concerned. Truhlar et al. have successfully used various semiempirical methods based on specific reaction parameters (SRP);[13−18] they introduce corrections interpolated with ab initio calculations (VTST-IC)[18−20] at stationary points. In this work, we used the same methodology to investigate intramolecular proton transfer in hydrogenoxalate anion (Figure 1) with the aid of a semiempirical method including SRP. This methodological approach at various computational levels is known as the "dual level" approximation. It is computationally more affordable and it allows more extensive exploration of the potential energy surface. This is quite important with a view to assessing tunneling, which was one of the primary purposes of this work. The dynamic results obtained were compared with those reported by other authors;[21−25] the little consistency among them, especially in terms of barrier height, suggests that this parameter has a marked effect on dynamics—particularly on tunneling. One other purpose of this work was to analyze the more significant contributions to kinetic isotopic effect (KIE)[26]—specifically, to the rate constant ratio, k_H/k_D.

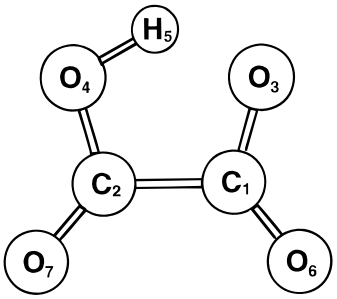

Figure 1. Atom numbering in hydrogenoxalate anion.

2. Computational Details

(a) Electronic Structure Calculations. To the authors' knowledge, the only static studies reported so far are those by

S1089-5639(98)00269-2 CCC: $15.00
Published on Web 04/04/1998

Bosch et al.[21,22] at the HF/3-21+G level and by Truong and McCammon[25] at the HF/6-31++G** and MP2/6-31++G** levels.

In this work, we improved the computational level by performing a static study of hydrogenoxalate anion at the QCISD level, using the 6-31++G** basis with full geometric optimization. The path of both the hydrogen and the deuterium transfer reaction was monitored at the MP2/6-31++G** level, using the algorithm of González-Schlegel[27] with a stepsize of 0.01 bohr amu$^{1/2}$ and Hessian calculations at 0.1 bohr amu$^{1/2}$. The algorithm yields the correct tangent vector and curvature vectors in the limit of small step size. The frequency of the Hessian calculations was enough, because we obtained the same rate constants using larger steps. The barrier height was corrected for the previously obtained QCISD/6-31++G** value. We chose a reduced mass—which converted mass-weighted Cartesian coordinates into mass-scaled coordinates—$\mu = 1$ amu in order to have both coordinate systems lead to the same results. This ab initio study, henceforward referred to as the *high level* (HL) approximation, is used as reference throughout the paper. Electronic structure calculations were performed by using the Gaussian 94 software package.[28]

Semiempirical calculations of barrier height and frequencies were corrected with the QCISD value and MP2 values, respectively. This approximation is widely known as the *dual level* (DL) approximation. It usually involved highly sophisticated ab initio calculations at stationary points and semiempirical calculations at other points on the potential energy surface. Unfortunately, standard semiempirical methods cannot be used as such in a dynamic study and require specific parametrization for adaptation to the reaction concerned. Standard semiempirical methods based on the neglect of diatomic differential overlap (NDDO) (e.g., MNDO,[29] AM1,[30] and PM3[31]) overestimate barrier heights and are thus inadvisable for this purpose. Truhlar et al. used these semiempirical methods with specific reaction parameters (NDDO−SRP)[13−18,20] to fit their results to those of a higher computational level. On the basis of this approach, in this work we used a modified version of the MNDO method previously developed by our group. Our version is specially parametrized for systems involving O−H···O bonding and is designated MNDO/H2. The underlying approximation is similar to that of the MNDO/H[33] and MNDO/M[34] methods; unlike these, however, it focuses more directly on the intramolecular hydrogen bond. It differs from the standard MNDO method in two main respects: (i) It replaces the empirical function $f(R_{OH})$ of core−core repulsion,

$$f(R_{OH}) = R_{OH} \exp(-\alpha_O R_{OH}) + \exp(\alpha_H R_{OH}) \qquad (1)$$

where R_{OH} is the O−H bond distance and α_O and α_H are two atomic parameters, by the function

$$f(R_{OH}) = A \exp[-\alpha(R_{OH} - \gamma)^2] \qquad (2)$$

with the following optimized parameter values:[32] $A = 0.2770$, $\alpha = 2.1655$, and $\gamma = 0.3597$. (ii) It assumes a zero value for the $f(R_{O-O})$, O−O being the oxygen atom pair involved in the hydrogen bond. Inasmuch as this semiempirical approximation has been parametrized for systems involving intramolecular hydrogen bonding, we can consider it a semiempirical method with system specific parameters and designate it NDDO SSP.[18] Based on the nomenclature criteria of ref 6a, the DL approximation used in this work can be designated QCISD/6-31++G**//MP2/6-31++G**//MNDO/H2. We used a suitable modification of the MORATE version 6.5 software package[35] to perform the semiempirical calculations required by the MNDO/H2 method.

(b) Dynamic Calculations. Intramolecular proton transfer in hydrogenoxalate anion and its deuterated species was studied in the context of the variational theory of the transition state (VTST),[11] using semiclassical tunneling (ST) corrections.[12]

In this study, the dual level scheme involved semiempirical MNDO/H2 calculations for all the nonstationary points and high level calculations for the stationary points. Concretely, the barrier height was corrected at the QCISD/6-31++G** level using two cutoff Gaussian functions, one for the reactant side and one for the product side of the MEP. Each cutoff Gaussian was solely determined by the corrections at the three stationary points (reactant, transition state, and product). The frequencies were also corrected following the scheme of ref 20, in this case at the MP2/6-31++G** level. Several approaches were used to take tunneling into account: zero curvature tunneling (ZCT),[11] centrifugal-dominant small-curvature semiclassical adiabatic ground-state (CD-SCSAG),[12] version 3 of the large curvature ground-state (LCG 3),[12,36] and microcanonical optimized multidimensional tunneling (μOMT).[14] In this last—at each energy—the transmission probability is taken as the maximum of two trial calculations, namely, the small curvature approximation (denoted by SCT and based on CD-SCSAG) and the large curvature method (denoted by LCT and based on LCG3). The ZCT approximation, the simplest scheme, assumes a negligible curvature along the reaction path and therefore the particle follows the MEP. In the SCT approximation the reaction path curvature is taken into account by calculation of a reduced mass that is used in computing the tunneling probability. As a consequence, the tunneling path is displaced from the MEP to a concave-side vibrational turning point in the direction of the internal centrifugal force. Finally, the LCT approximation involves a straight-line trajectory between the atoms binding the proton before and after the transfer. This last approximation was mainly developed for reactions that involve light atoms, because in such a case the transferred particle follows a path which is far from the MEP. The LCT method needs energy calculations along the straight path, which were evaluated with the MNDO/H2 method and corrected with a quadratic function that includes HL calculations.[20]

In high level calculations, tunneling was only evaluated by using the ZCT and SCT approximations as provided by the program POLYRATE version 6.5.[37]

The kinetic isotopic effect was evaluated as the ratio of the rate constant for hydrogen (k_H) to that for deuterium (k_D), using the contributions of tunneling, translation, rotation, vibration, and variational effects.[26,38] The contribution of translation was unity since the reaction was unimolecular.

3. Results and Discussion

(a) Minima and Transition States. Tables 1 and 2 show the geometries and barrier heights, respectively, obtained at various ab initio levels and with the MNDO/H2 method.

The difference between the barrier heights obtained with fully optimized MP2 and fully optimized QCISD is substantial. However, that difference is only 0.07 kcal/mol when we compare the single point QCISD calculations (over the MP2 geometry) against the complete QCISD calculations. That is a consequence of the similarity between both geometries, which suggests that the electron correlation used at the MP2 level was inadequate and testifies to its significant role in this kind of reaction. It is also confirmed by isolated MP4SDQ/6-31++G**

TABLE 1: Main Geometric Parameters for the Minimum and Transition State of Hydrogenoxalate Anion[a]

	level (basis)				
		HF		MP2	QCISD
	MNDO/H2	3-21+G[b]	6-31++G**[c]	6-31++G**[c]	6-31++G**
			Minimum		
C_1C_2	1.56	1.57	1.577	1.575	1.5823
C_1O_3	1.27	1.27	1.243	1.283	1.2768
C_2O_4	1.36	1.36	1.329	1.358	1.3579
O_4H_5	0.99	0.98	0.958	1.001	0.9900
O_3O_4	2.42	2.51	2.515	2.497	2.5158
$C_2C_1O_3$	109.6	110.9	111.3	110.9	111.05
$C_1C_2O_4$	108.3	110.7	111.3	109.8	110.41
$C_2O_4H_5$	108.0	107.7	104.2	98.9	100.55
			Transition State		
C_1C_2	1.55	1.58	1.573	1.574	1.5811
C_2O_4	1.31	1.32	1.283	1.317	1.3141
O_4H_5	1.26	1.23	1.201	1.224	1.2198
O_3O_4	2.25	2.30	2.276	2.328	2.3212
$C_1C_2O_4$	105.4	105.8	105.9	106.8	106.68
$C_2O_4H_5$	101.3	95.6	92.7	91.1	91.56
Δr_{O-O}[d]	0.17	0.21	0.239	0.169	0.1946

[a] Bond distances in angstroms and angles in degrees. [b] Reference 21. [c] Reference 25. [d] Distance O_3-O_4.

TABLE 2: Classical ($\Delta V^{\neq}$) and Vibrationally Adiabatic Ground-State Barrier ($\Delta V_a^{G\neq}$) in kcal/mol, for Proton Transfer in Hydrogenoxalate Anion

level/basis	$\Delta V^{\neq}$	$\Delta V_a^{G\neq}$
MNDO/H2	3.90	2.74(H) 3.20(D)
HF/3-21+G[a]	8.34	5.84(H) 6.82(D)
HF/6-31++G**[b]	9.26	6.50(H) 7.42(D)
MP2/6-31++G**[b]	3.12	0.82(H)[c] 1.55(D)[c]
MP4(SDQ)//MP2/6-31++G**	4.68	
QCISD//MP2/6-31++G**	4.78	
QCISD/6-31++G**	4.85	2.55(H)[c] 3.28(D)[c]

[a] Reference 21. [b] Reference 25. [c] Values obtained by correcting the zero-point energy with MP2/6-31++G** frequencies.

calculations, which exhibited a similar trend (see Table 2). Relative to the HF results, C_1O_3 and OH bond distances were longer and the $C_2O_4H_5$ bond angle smaller, both at the minimum and in the transition state, when electron correlation was included. All these angles and bond lengths are closely related to the proton transfer, so they are especially significant to and strongly influential on barrier height.[8,39−41] One other influential geometric parameter in this context is the difference in the distance of the oxygen atoms that take part in the transfer between the minimum and the transition state (Δr_{O-O} in Table 1); as a rule, the barrier height increases with increasing Δr_{O-O}, as was indeed our case.[42] In that context, the MNDO/H2 semiempirical method provided acceptable geometries. This method was parametrized in such a way as to reproduce the height of the intramolecular proton transfer barrier, so one could reasonably expect it to provide acceptable distances and angles for the hydrogen bond. Although the $C_2O_4H_5$ angles thus obtained were much wider than those provided by MP2 and HF, OH bond distances and Δr_{O-O} values were similar to their MP2 counterparts; this is reflected in a barrier height of only 3.90 kcal/mol, which is between the MP2 and QCISD values.

(b) Frequencies and Zero-Point Energies. Table 3 gives the frequencies for stationary points at the MP2/6-31++G** level. Frequency ω_1 corresponds to OH bond stretching, ω_2 and ω_3 correspond to C_1O_6 and C_2O_7 stretching vibrations,

TABLE 3: Vibrational Frequencies (in cm^{-1}) and Zero-Point Energy (ZPE in kcal/mol) Calculated by Using the MP2/6-31++G Method and the MNDO/H2 Semiempirical Method[a]**

	MP2/6-31G**		MNDO/H2	
frequency	minimum	TS	minimum	TS
ω_1	3245(a′)	2075(*a*1)	2681	2307
ω_2	1802(*a*′)	1791(*b*2)	2170	2131
ω_3	1735(*a*′)	1745(*a*1)	2106	2107
ω_4	1432(*a*′)	1325(*a*1)	1621	1672
ω_5	1328(*a*′)	1299(*b*2)	1558	1614
ω_6	1138(*a*′)	863(*a*1)	1359	979
ω_7	934(*a*″)	1266(*b*1)	814	967
ω_8	827(*a*′)	746(*b*2)	925	749
ω_9	786(*a*″)	785(*a*2)	736	825
ω_{10}	690(*a*′)	714(*a*1)	667	707
ω_{11}	566(*a*′)	604(*b*2)	593	595
ω_{12}	477(*a*″)	480(*b*1)	463	475
ω_{13}	423(*a*′)	336(*a*1)	441	361
ω_{14}	296(*a*′)	1072*i*(*a*2)	252	1007i
ω_{15}	92(*a*″)	133(*a*2)	100	144
ZPE	22.55	20.24	23.53	22.37

[a] Symmetry labels are given in parentheses. All the frequencies are correlated with those obtained at the MP2 equilibrium configuration.

respectively, ω_4 and ω_5 correspond to C_1O_3 and C_2O_4 stretching vibrations, respectively, ω_7 corresponds to out-of-plane bending for hydrogen; ω_9 and ω_{12} correspond to carbon wagging, ω_6 and ω_8 correspond to OCO bending; ω_{10}, ω_{11}, and ω_{13} correspond to combinations of various in-plane movements of the heavier atoms, ω_{14} correspond to the reaction coordinate, and ω_{15} corresponds to twisting about the C−C bond. Despite the substantial changes in frequencies ω_4, ω_6, and ω_7, it was the OH stretching frequency that underwent the greatest variation along the reaction path (more than 1000 cm^{-1} between the reactant and the transition state). HF calculations grossly overestimate both ω_1 at the minimum and the imaginary frequency relative to MP2 calculations (see Table 4). Usually, this results in higher energy barriers and longer reaction paths from HF calculations. Differences in the frequencies affect the zero-point energy and hence the vibrationally adiabatic ground-state potential, defined as

$$V_a^G(s) = V_{MEP}(s) + \epsilon_{int}^G(s) \quad (3)$$

TABLE 4: OH Streching Frequency (ω_1 in cm^{-1}), Reaction Coordinate Frequency (ω_{14} in cm^{-1}), and Zero-Point Energy (ZPE in kcal/mol) at Minimum and Transition State, Obtained at Different Computational Levels

	ω_1		ω_{14}		ZPE	
level/basis	minimum	TS	minimum	TS	minimum	TS
HF/3-21+G[a]	3642	2271	320	1511i	23.89	21.39
HF/6-31++G**[b]	3913	2287	368	1649i	25.35	22.59
MP2/6-31++G**	3245	2075	296	1072i	22.55	20.24

[a] Reference 21. [b] Reference 25.

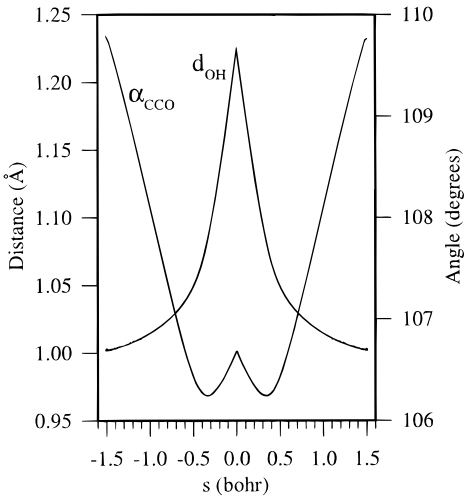

Figure 2. Variation of the O−H distance, d_{OH}, and $C_1C_2O_4$ angle, α_{CCO}, along the MEP.

as well as $\Delta V_a^{G\neq}$, defined as

$$\Delta V_a^{G\neq} = V_a^{G}(s=0) - V_a^{G}(s=s^R) \qquad (4)$$

where $\epsilon_{int}^{G}(s)$ denotes the contribution of the zero point energy of the transverse modes to the reaction path and s^R the location of the reactants. The difference in zero-point energies can be significant for reactions with low barrier heights;[25,39,43,44] also, it can alter the transmission factors for different isotopes and hence the contribution of tunneling to kinetic isotopic effect. Specifically, we found a zero point energy difference of 0.19 kcal/mol between HF/3-21+G and MP2 calculations and of 0.45 kcal/mol between HF/6-31++G** and MP2 calculations (Table 4).

The MNDO/H2 semiempirical method provides acceptable frequencies; however, it gives too low of a OH stretching frequency. The differences in that frequency and the other transverse modes to the reaction path can be corrected by interpolation with MP2 frequencies at stationary points, as shown in the following section. The imaginary frequency—reaction coordinate—is similar to that of MP2 and so should the barrier width along the MEP be as a result.

(c) Reaction Path. The reaction path for the proton transfer was taken to be the minimum energy path (MEP) obtained from MP2/6-31++G** calculations. Its length was found to be 3.02 bohr for the transfer of hydrogen and 3.36 bohr for that of deuterium (where the values just quoted equal $2|s^R|$, due to the symmetry of the molecule).

Usually, this type of reaction initially involves molecular rearrangement—essentially about the heavy atoms—and, nearer the transition state, proton transfer.[8,39] This circumstance also holds in our case. So, as shown in Figure 2, $C_1C_2O_4$ has already changed by more than 80% at the halfway point on the reaction path from the minima to the transition state ($s = -0.75$ bohr).

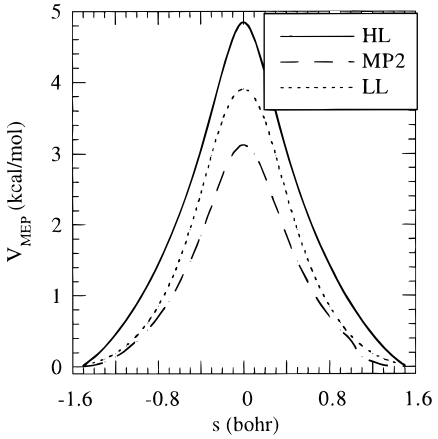

Figure 3. Variation of the MEP potential along the reaction coordinate at different computational levels. HL, MP2, and LL denote high level, MP2/6-31++G**, and low level (MNDO/H2) calculations, respectively.

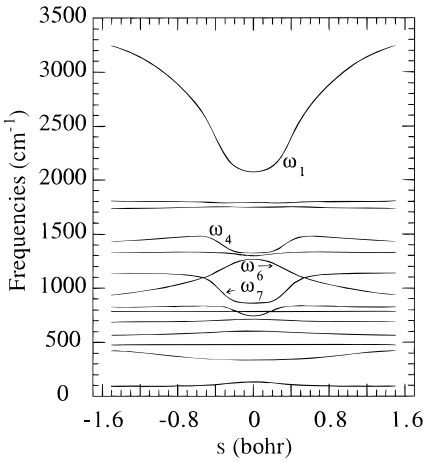

Figure 4. Generalized frequencies at the MP2/6-31++G** level along the reaction coordinate.

This is the coordinate that, involving heavy atoms, suffers a more substantial change along the reaction path. As regards the OH bond distance, it remains virtually unchanged in the range from $s = s^R$ to $s = -0.5$ bohr. Therefore, the transfer takes place at a reaction path length of about 1.0 bohr, which is merely one-third of the overall MEP length. Consequently, because changes in the OH bond distance entail a high energy cost and take place over a narrow range, the MEP will be quite sharp in this zone.

The MEP length provided by the semiempirical method was virtually coincident with the MP2 length (Figure 3), so no correction in this respect was required. In any case, we corrected the barrier height to obtain the QCISD value.

The generalized frequencies along the reaction coordinate (Figure 4) at MP2 level remained virtually unchanged up to about halfway on the reaction path from the minimum of the transition state ($s = -0.75$ bohr). Beyond that point, the frequencies more closely related to the transfer varied significantly because this is the zone where vibrational modes are most closely coupled to the reaction path. Figure 5 shows the curvature of the reaction path, $\kappa(s)$. The most closely coupled modes are OH stretch (ω_1), $C_1O_3-C_2O_4$ stretching (ω_4, of a_1 symmetry in the transition state) and OCO−OCO bending (ω_6, of a_1 symmetry in the transition state). The dynamic coupling constants[45] ($B_{k,F}$), between these three modes ($k = 1, 4, 6$) and the reaction coordinate account for over 90% of the curvature

TABLE 5: Rate Constants (in s^{-1}) for the Intramolecular Transfer of Hydrogen and Deuterium in Hydrogenoxalate Anion and Ratios between the Constants (with and without Tunneling)

	H			D			k_H/k_D[b]		
T, K	TST	TST/ZCT	TST/SCT	TST	TST/ZCT	TST/SCT	TST	TST/ZCT	TST/SCT
200	4.86(9)[a]	2.03(10)	5.88(10)	7.19(8)	2.04(9)	4.98(9)	6.76	9.94	11.76
250	2.02(10)	5.27(10)	1.11(11)	4.30(9)	8.21(9)	1.38(10)	4.70	6.39	7.85
300	5.30(10)	1.05(11)	1.82(11)	1.43(10)	2.23(10)	3.17(10)	3.71	4.71	5.75
400	1.79(11)	2.67(11)	3.71(11)	6.44(10)	8.24(10)	9.92(10)	2.78	3.22	3.73
500	3.76(11)	4.87(11)	6.07(11)	1.60(11)	1.87(11)	2.10(11)	2.35	2.61	2.89

[a] Powers on 10 are given in parentheses. [b] The classical contribution of rotation to the k_H/k_D ratio was 1.01 at every temperature.

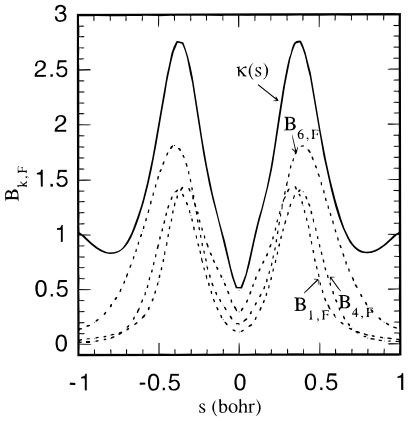

Figure 5. Variation of the $B_{1,F}$, $B_{4,F}$, and $B_{6,F}$ couplings along the reaction coordinate. The total curvature of the reaction path, $\kappa(s)$ is also shown (—).

TABLE 6: Transmission Factors at HL for Both Isotopes

	κ_H			κ_D			κ_H/κ_D		
T(K)	0-ZCT[a]	ZCT	SCT	0-ZCT[a]	ZCT	SCT	0-ZCT[a]	ZCT	SCT
200	1.19	4.18	12.09	2.07	2.84	6.93	0.57	1.47	1.74
250	1.12	2.60	5.47	1.61	1.91	3.27	0.69	1.36	1.67
300	1.08	1.98	3.43	1.40	1.56	2.22	0.77	1.27	1.55
400	1.04	1.49	2.07	1.21	1.28	1.54	0.86	1.16	1.34
500	1.03	1.30	1.61	1.13	1.17	1.31	0.91	1.11	1.23

[a] Reference 25.

of the reaction path, $\kappa(s)$, so the other modes are scarcely coupled to the MEP. A maximum at $-0.4 < s < -0.3$ bohr is observed in the reactant zone (and at $0.3 < s < 0.4$ bohr in the product zone since the reaction path is symmetric). Because $B_{1,F}$, $B_{4,F}$, and $B_{6,F}$ are significant, vibrational excitation in these modes will lead to a substantially increased rate constant.

(d) High Level (HL) Dynamic Calculations. Table 5 gives the rate constants for the transfer of hydrogen and deuterium, as well as the corresponding ratios between the two HL constants. The rate constants were calculated in the light of the canonical variational theory (CVT) of the transition state.[1] However, no variational effects were encountered over the temperature range studied, so the results shown are those obtained on the basis of the conventional transition state theory (TST).

Regarding KIE contributions, that of vibration was the most important contribution (Table 5) but was smaller than predicted by Truong and McCammon;[25] for example, our KIE value at 200 K was 1.5 times smaller, probably because these authors used HF/6-31++G** frequencies. However, our greatest difference from their calculations is in the relative significance of tunneling with the different isotopes involved (Table 6). The tunneling effect in our calculations is larger for both isotopes and the tunneling increases the KIE, while in their calculations tunneling decreases the KIE. These authors used the MP2/6-31++G** barrier height with HF/6-31++G** frequency calculations at stationary points and dealt with tunneling from the 0-ZCT approximation since the barrier at the MP2 level was quite low. They observed an "anomalous isotope effect" as a result of the differential contribution of the individual isotopes to the zero-point energy. This is very interesting and signifies one more case when tunneling need not increase KIE.[25,39,46] However, we believe QCISD calculations provide a more correct barrier height.

We evaluated the contribution of tunneling to HL rate constants using the zero curvature (ZCT) and small curvature methods (SCT) and obtained the transmission factor, κ, listed in Table 6. κ_{HL}^{SCT} values were greater than κ_{HL}^{ZCT} values, both for hydrogen and for deuterium. This can be ascribed to the curvature of the reaction path, which decreases the effective mass (see ref 11) and hence the action integral, thereby increasing the probability of tunneling and, consequently, the transmission factor. The presence of curvature is a necessary condition for the proton to follow a path other than the MEP; the OH stretching mode (ω_1), which is intimately coupled to the reaction path and involves proton motion only, will tend to favor more rectilinear—and hence shorter—trajectories since these involve no motion of the heavy atoms. This mode, and modes ω_4 and ω_6, are symmetric in the transition state and tend to favor the transfer and tunneling and increase the kinetic isotopic effect (KIE); on the other hand, antisymmetric modes such as ω_7 hinder the transfer and the tunneling and decrease the KIE.[25,39,47,48]

The dynamic calculations of Bosch et al.,[21,23,24] based on a two-dimensional surface at the HF/3-21+G level, suggest that the hydrogen transfer is likely to follow a path more rectilinear than the MEP. These results and the presence of modes intimately coupled to the reaction path may require the use of large curvature calculations (LCT), which prompted us to employ dual level methodology for their evaluation.

(e) Dual Level (DL) Dynamic Calculations. We used the MNDO/H2 modification as described in section 2 for dynamic calculations. We chose to correct the barrier height rather than alter the semiempirical method proper in order to ensure that the breadth of the reaction path would remain constant—this was advisable because such a breadth was similar to the MP2 value. These results are consistent with the imaginary frequencies obtained in both cases as they are very similar. The orthonormal frequencies to the MEP were accurately interpolated; for example, the OH stretching mode (ω_1), which was that undergoing the most marked changes along the reaction path and was subject to a substantial error relative to MP2 calculations, provided an acceptable result (Figure 6). The MEP calculated at the HL and DL levels was superimposed, so it is not shown. The $V_a^G(s)$ values provided by the two methodologies depart in the zone of maximum curvature as a result of more abrupt changes in the frequencies of the ab initio surface relative to the semiempirical frequencies in that zone; consequently, interpolation at that point was not fully efficient (Figure

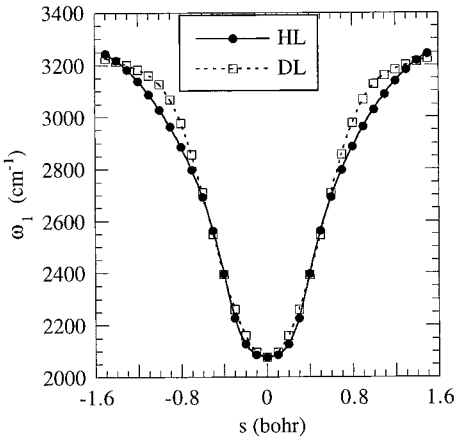

Figure 6. Variation of the OH stretching frequency, ω_1, along the MEP, at both high level (HL) and dual level (DL). Circles and squares represent the points where the Hessian is available.

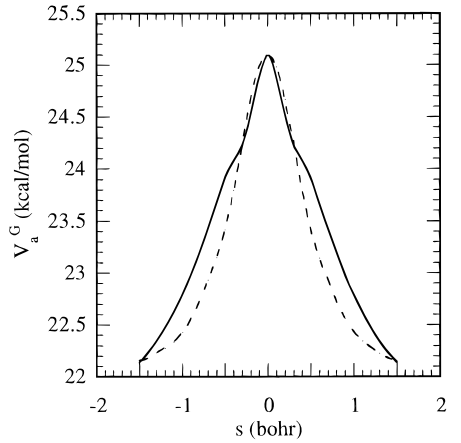

Figure 7. Variation of the vibrationally adiabatic ground-state potential, V_a^G, along the MEP for proton transfer in hydrogenoxalate anion. The solid line represents HL calculations and the broken line DL calculations.

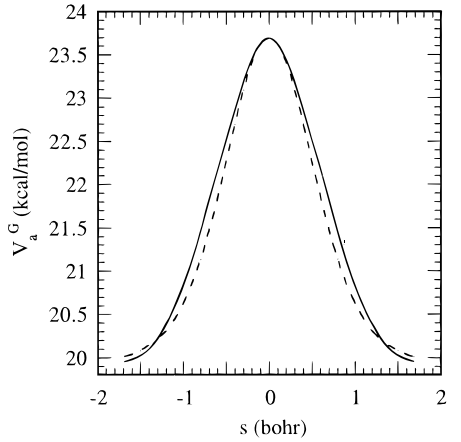

Figure 8. Variation of the vibrationally adiabatic ground-state potential, V_a^G, along the MEP for the deuterium transfer in hydrogenoxalate anion. The solid line represents HL calculations and the broken line DL calculations.

7). This was not the case with deuterium transfer because the curvature was smaller and so were thus frequency changes (Figure 8).

Because DL calculations involved HL corrections at stationary points and no variational effects were observed over the temperature range studied, the differences between HL and DL calculations must be exclusively due to tunneling. κ_{HL}^{ZCT} transmission factors (Table 6) were smaller than κ_{DL}^{ZCT} factors (Table 7), both for hydrogen and for deuterium; at low temperatures, differences were significant but never exceeded 11% and 16% for hydrogen and deuterium, respectively, not even at $T = 250$ K. The SCT transmission factors were more consistent and virtually identical throughout the temperature range studied. Because the differences between κ_{HL} and κ_{DL} values were not too large, we believe they must be—at least qualitatively—preserved in large curvature transmission factors. The LCT transmission factors are smaller than SCT factors, which suggests that small curvature calculations on this reaction are adequate (Table 7) and confirms the results discussed in section 3d. The $\kappa_{DL}^{\mu OMT}$ transmission factors,[14] an alternative to the least-action method (LAG),[49] are identical with κ_{DL}^{SCT} factors.

TABLE 7: Transmission Factors at DL for Both Isotopes

	κ_H[a]			κ_D[a]			κ_H/κ_D		
T, K	ZCT	SCT	LCT	ZCT	SCT	LCT	ZCT	SCT	LCT
200	5.20	12.25	6.47	3.64	6.75	3.90	1.43	1.81	1.66
250	2.88	5.19	3.26	2.21	3.19	2.28	1.30	1.63	1.43
300	2.09	3.18	2.25	1.72	2.18	1.74	1.22	1.46	1.29
400	1.51	1.93	1.57	1.35	1.52	1.35	1.12	1.27	1.16
500	1.30	1.52	1.33	1.21	1.30	1.21	1.07	1.17	1.10

[a] The $\kappa^{\mu OMT}$ value was always the same as the κ^{SCT} value.

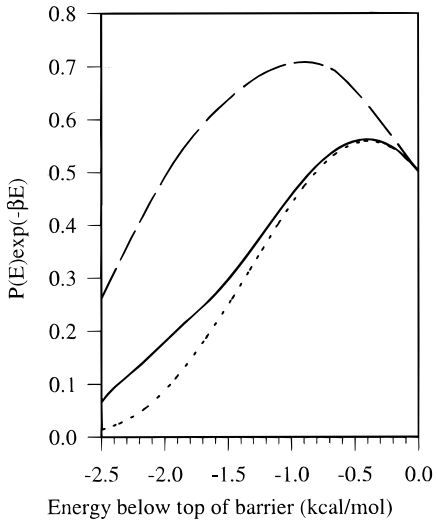

Figure 9. Thermally averaged transmission probability at 300 K in the proton transfer of hydrogenoxalate anion. Probability calculated with ZCT (•••), SCT (- - -), and LCT (—).

The LCT transmission factors are smaller than SCT factors, which suggests that small curvature calculations on this reaction are adequate (Table 7) and confirms the results discussed in section 3d. The $\kappa_{DL}^{\mu OMT}$ transmission factors,[14] an alternative to the least-action method (LAG),[49] are identical with κ_{DL}^{SCT} factors.

Therefore, both the proton and deuterium follow a path close to that of minimum energy rather than a more rectilinear trajectory in this transfer reaction. The divergence between our results and those of Bosch et al. may be the result of the difference between the HF and QCISD barrier heights (8.34 and 4.85 kcal/mol, respectively).

(f) Representative Tunneling Energy and Tunneling Path. The term "representative tunneling energy" (E_{rep}) is used to designate the energy at which the product of the Boltzmann factor by the tunneling probability is maximal.[50] Figure 9 shows the dual level representative tunneling energy for hydrogen at 300 K as calculated by using the three approximations (ZCT, SCT, and LCT). When available, HL values are given in brackets below. The E_{rep} value is reached at $s = -0.31$ (-0.33) bohr with SCT, $s = -0.19$ (-0.21) bohr with ZCT, and $s = -0.19$ bohr with LCT (Table 8). The area enclosed by the small curvature method in Figure 9 is much greater than those provided by the other two methods; this accounts for its

TABLE 8: Representative Tunneling Energy[a]

	E_{rep}			s_l		
T, K	ZCT	SCT	LCT	s_{ZCT}	s_{SCT}	s_{LCT}
250	24.44	23.60	24.40	−0.25	−0.45	−0.26
300	24.70	24.17	24.69	−0.19	−0.31	−0.19
400	24.99	24.70	24.98	−0.09	−0.19	−0.09

[a] E_{rep} in kcal/mol. Reaction coordinate in the pretunneling configuration (s_l in bohr). Calculations were performed at the dual level.

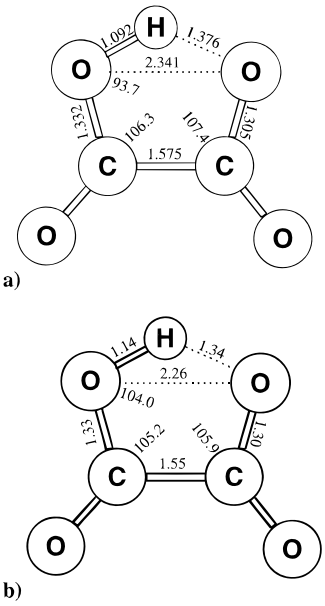

Figure 10. Pretunneling geometries obtained from SCT transmission factors at 300 K: (a) HL; (b) MNDO/H2.

increased transmission factor and hence for the greater probability of its path. The most probable tunneling configuration occurs at lower energies in SCT calculations—specifically, at 0.92 (0.98), 0.39 (0.56), and 0.40 kcal/mol below the barrier with SCT, ZCT, and LCT, respectively (Figure 9). The pretunneling (s_l) geometries at $s = -0.31$ (−0.33) bohr and the posttunneling (s_r) geometries at $s = 0.31$ bohr are those where $V_a^G(s_l)$ and $V_a^G(s_r)$ equal the representative tunneling energy. The HL geometry at $s = s_l$ is shown in Figure 10, together with the pretunneling geometry obtained from DL calculations. The interval between pretunneling and posttunneling configurations is called the "representative tunneling path". In our case, this path joins two symmetric geometries belonging to the C_s point group. The O_4H_5 distance in the pretunneling geometry (and the O_3H_5 distance in the posttunneling geometry) is 1.14 (1.092) Å; in the equilibrium configuration, such a distance is 0.99 (1.001) Å. Notwithstanding the substantial differences between DL and HL pretunneling geometries, some of the parameters relevant to the transfer (e.g., the OH bond distance and Δr_{O-O}) follow the same trend, so the differences in E_{rep} and in the representative tunneling path are relatively small. In both cases, the O_4H_5 distance is far from its value in the transition state; this suggests that a substantial portion of the transfer follows the tunneling path, which is bound by the small curvature approximation. On the other hand, the O_3O_4 distance is virtually identical with that in the transition state, which confirms that the rearrangement of heavy atoms to favor the transfer has taken place by then. Finally, to ascertain the accuracy of the SCT approximation to this reaction, we considered the angle between the tunneling path and the MEP at $s = s_l$, which was only 21° and 12° at 250 and 300 K, respectively. This confirms the previously assumed small curvature.

4. Conclusions

The barrier height for the intramolecular proton transfer in hydrogen oxalate ion obtained at the QCISD/6-31++G** level with full geometric optimization was 4.85 kcal/mol and hence substantially higher than its MP2 counterpart. The transfer along the MEP initially involves a rearrangement of the molecular geometry—largely about the heavy atoms—to favor the process. Subsequently, the proton is transferred over a fairly short MEP interval.

High level dynamic calculations for both hydrogen and deuterium suggest that the greatest contribution to isotopic effect is that of vibration. On the other hand, tunneling was adequately described by the SCT approximation, even though it revealed that some modes were intimately coupled to the path. At low temperatures, the transfer follows in an important portion the tunneling path. It was also observed that the tunneling path is not very curved regarding the MEP. A comparison of the QCISD and HF barriers reveals that the latter approximation provides overestimated barriers with a seemingly strong influence on the tunneling trajectory. MP2 barriers exhibit the opposite effect, i.e., they underestimate barriers and tunneling. Based on the results obtained in proton transfer reactions, we believe barrier height is one of the most influential parameters on the dynamics, even though others such as frequencies and the zero-point energy are also significantly influential. While one cannot rule out the use of ab initio methods without electron correlation or of MP2 methods to determine barrier heights, the results they provide should be taken reservedly.

Finally, we have demonstrated the effectiveness of specially parametrized semiempirical methods based on the dual level approximation and *direct dynamics* calculations based solely on electronic structure using no analytical potential energy surface. Despite its constraints, the MNDO/H2 modification can be a useful tool in this context, particularly with bulky systems, which are unaffordable to pure ab initio calculations.

Acknowledgment. M.A.R., J. R.-O., and A. F.-R. thank Professor Truhlar for advice in obtaining the programs POLYRATE and MORATE, the Centro de Supercomputación de Galicia (CESGA) for access to its computational facilities, and Spain's Ministry of Education and Science for financial support of this work via Project PB94-0620. A.F.-R. is also grateful to the Xunta de Galicia for additional support in the form of a grant.

References and Notes

(1) Bell, R. P. *The Tunnel Effect in Chemistry*; Chapman & Hall: London, 1980.

(2) Caldin, E. F.; Gold, V. *Proton-transfer Reactions*; Chapman & Hall: London, 1975.

(3) Stewart, R. *The Proton: Applications to Organic Chemistry*; Academic: Orlando, 1985.

(4) Bountis, T. *Proton Transfer in Hydrogen-Bonded Systems*; NATO ASI Series (B291); Plenum Press: New York and London, 1991.

(5) Truhlar, D. G. *The Reaction Path in Chemistry; Current approaches and Perspectives*; Heindrich, D., Ed.; Kluwer: Dordrecht, 1995; pp 229−255 and references therein.

(6) (a) Corchado, J. C.; Espinosa-García, J.; Hu, W.-P.; Rossi, Y.; Truhlar, D. G. *J. Phys. Chem.* **1995**, *99*, 687. (b) Espinosa-García, J.; Corchado, J. *J. Chem. Phys.* **1994**, *101*, 1333. (c) Espinosa-García, J.; Corchado, J.; *J. Chem. Phys.* **1994**, *101*, 8700.

(7) Truong, T. N. *J. Chem. Phys.* **1994**, *100*, 8014.

(8) Bell, R. L.; Truong, T. N. *J. Chem. Phys.* **1994**, *101*, 10 442.

(9) Villà, J.; González-Lafont, A.; Lluch, J. M. *J. Phys. Chem.* **1996**, *100*, 19 389.

(10) Hu, W.-P.; Truhlar, D. G. *J. Am. Chem. Soc.* **1995**, *117*, 10 726.

(11) Truhlar, D. G.; Isaacson, A. D.; Garrett, B. C. In *Theory of Chemical Reaction Dynamics*; Baer, M., Ed.; Chemical Rubber: Boca Raton, FL, 1985; Vol. 4, pp 65−137 and references therein.

(12) Lu, D.-h.; Truong, T. N.; Melissas, V. S.; Lynch, G. C.; Liu, Y.-P.; Garrett, B. C.; Steckler, R.; Isaacson, A. D.; Rai, S. N.; Hancock, G. C.; Lauderdale, J. G.; Joseph, T.; Truhlar, D. G. *Comput. Phys. Commun.* **1992**, *71*, 235.

(13) González-Lafont, A.; Truong, T. N.; Truhlar, D. G. *J. Phys. Chem.* **1991**, *95*, 4618.

(14) Liu, Y.-P.; Lu, D.-h.; González-Lafont, A.; Truhlar, D. G.; Garrett, B. C. *J. Am. Chem. Soc.* **1993**, *115*, 7806.

(15) Liu, Y.-P.; Lynch, G. C.; Truong, T. N.; Lu, D.-h.; Truhlar, D. G.; Garrett, B. C. *J. Am. Chem. Soc.* **1993**, *115*, 2408.

(16) Kim, Y. *J. Am. Chem. Soc.* **1996**, *118*, 1522.

(17) Hu, W.-P.; Truhlar D. G. *J. Am. Chem. Soc.* **1996**, *118*, 860.

(18) Chuang, Y.-Y.; Truhlar, D. G. *J. Chem. Phys.* **1997**, *107*, 83.

(19) (a) González-Lafont, A.; Truong, T. N.; Truhlar, D. G. *J. Phys. Chem.* **1991**, *95*, 8875. (b) Nguyen, K. A.; Rossi, Y.; Truhlar, D. G. *J. Chem. Phys.* **1995**, *103*, 5522.

(20) Hu, W.-P.; Liu, Y.-P.; Truhlar, D. G. *J. Chem. Faraday Trans.* **1994**, *90*, 1715.

(21) Bosch, E.; Moreno, M.; Lluch, J. M.; Bertrán, J. *J. Chem. Phys.* **1990**, *93*, 5685.

(22) Bosch, E.; Moreno, M.; Lluch J. M. *Can. J. Chem.* **1992**, *70*, 100.

(23) Bosch, E.; Moreno, M.; Lluch, J. M. *Chem. Phys. Lett.*. **1992**, *196*, 73.

(24) Bosch, E.; Moreno, M.; Lluch, J. M. *Chem. Phys.* **1992**, *159*, 99.

(25) Truong, T. N.; McCammon, A. *J. Am. Chem. Soc.* **1991**, *113*, 7504.

(26) Melander, N.; Saunders, W. H., Jr. In *Reaction Rates of Isotopic Molecules*; Wiley: New York, 1980.

(27) (a) González, C.; Schlegel, H. B. *J. Phys. Chem.* **1989**, *90*, 2154. (b) Gonzalez, C.; Schlegel, H. B. *J. Phys. Chem.* **1990**, *94*, 5523.

(28) Frisch, M. J.; Trucks, G. W.; Schlegel, H. B.; Gill, P. M. W.; Johnson, N. G.; Robb, M. A.; Cheeseman, J. R.; Keith, T.; Petersson, G. A.; Montgomery, J. A.; Raghavachari, K.; Al-Laham, M. A.; Zakrzewski, V. G.; Ortiz, J. V.; Foresman, J. B.; Cioslowski, J.; Stefanov, B. B.; Nanayakkara, A.; Challacombe, M.; Peng, C. Y.; Ayala, P. Y.; Chen, W.; Wong, M. W.; Andres, V; Replogle, E. S.; Gomperts, R.; Martin, R. L.; Fox, D. J.; Binkley, J. S.; Defrees, D. J.; Baker, J.; Stewart, V.; Head-Gordon, M.; Gonzalez, C.; Pople, J. A. *Gaussian 94, Revision C.3*; Gaussian, Inc.: Pittsburgh, PA, 1995.

(29) Dewar, M. J. S.; Thiel, W. J. *J. Am. Chem. Soc.* **1977**, *99*, 4899.

(30) Dewar M. J. S.; Zoebisch, E. G.; Healy, E. F.; Stewart, J. J. P. *J. Am. Chem. Soc.* **1985**, *107*, 3902.

(31) Stewart, J. J. P. *J. Comput. Chem.* **1989**, *10*, 221.

(32) (a) Ríos, M. A.; Rodríguez, J. *J. Comput. Chem.* **1992**, *13*, 860. (b) Rodríguez, J. *J. Comput. Chem.* **1994**, *15*, 183.

(33) Burstein, K. Y.; Isaev, A. N. *Theor. Chim. Acta*, **1984**, *64*, 397.

(34) (a) Bliznyuk, A. A.; Voityuk A. A. *Theor. Chim. Acta* **1987**, *72*, 223. (b) Bliznyuk, A. A.; Voityuk A. A. *J. Mol. Struct. (THEOCHEM)* **1988**, *164*, 343.

(35) Hu, W.-P.; Lynch, G. C.; Liu, Y.-P.; Rossi, I.; Stewart, J. J. P.; Steckler, R.; Garrett, B. C.; Isaacson, A. D.; Lu, D.-h.; Melissas, V. S.; Truhlar, D. G. MORATE 6.5; University of Minnesota: Minneapolis, MN 1995.

(36) Garrett, B. C.; Joseph, T.; Truong, T. N.; Truhlar, D. G. *Chem. Phys.* **1989**, *136*, 271.

(37) Steckler, R.; Hu, W.-P.; Liu, Y.-P.; Lynch, G. C.; Garrett, B. C.; Isaacson, A. D.; Lu, D.-h.; Melissas, V. S.; Rai, S. N.; Hancock, G. C.; Lauderdale, J.; Joseph, T.; Truhlar, D. G. POLYRATE 6.5, University of Minnesota, Minneapolis, MN, 1995.

(38) Lu, D.-h.; Maurice, D.; Truhlar, D. G. *J. Am. Chem. Soc.* **1990**, *112*, 6206.

(39) Fernández-Ramos, A.; Rodríguez-Otero, J.; Ríos, M. A. *J. Chem. Phys.* **1997**, *107*, 2407.

(40) (a) Cybulsky, S. M.; Scheiner, S. *J. Am. Chem. Soc.* **1989**, *111*, 23. (b) Scheiner, S. *J. Mol. Struct. (THEOCHEM)* **1994**, *307*, 65.

(41) Duan, X.; Scheiner, S. *J. Am. Chem. Soc.* **1992**, *114*, 5849.

(42) Ríos, M. A.; Rodríguez J. *J. Mol. Struct.(THEOCHEM)* **1991**, *228*, 149. (b) Graña, A. M.; Ríos, M. A.; Rodríguez, J. *Struct. Chem.* **1991**, *2*, 575.

(43) Huskey, W. P. *J. Am. Chem. Soc.* **1996**, *118*, 1663.

(44) García-Viloca, M.; González-Lafont, A.; Lluch, J. M. *J. Am. Chem. Soc.* **1997**, *119*, 1081.

(45) Miller, W. H.; Handy, N. C.; Adams, J. E. *J. Chem. Phys.* **1980**, *72*, 99.

(46) Storer, J. W.; Houk, K. N. *J. Am. Chem. Soc.* **1993**, *115*, 10 426.

(47) Bell, R. L.; Truong, T. N. *J. Phys. Chem.* **1997**, *101*, 7802.

(48) Smedarchina, Z.; Fernández-Ramos, A.; Ríos, M. A. *J. Chem. Phys.* **1997**, *106*, 3956.

(49) (a) Garrett,. C.; Truhlar, D. G. *J. Chem. Phys.* **1983**, *79*, 4931. (b) Lynch, G. C.; Truhlar, D. G.; Garrett, B. C. *J. Chem. Phys.* **1989**, *90*, 3102. (c) Allison, T. C.; Lynch, G. C.; Truhlar, D. G.; Gordon, M. S. *J. Phys. Chem.* **1996**, *100*, 13 575.

(50) Kim, Y.; Truhlar, D. G.; Kreevoy, M. M. *J. Am. Chem. Soc.* **1991**, *113*, 7837.